Supplementary Material (ESI) for *PCCP*

SUPPLEMENTARY DATA

Dynamic mixing processes in spin triads of "breathing crystals" $Cu(hfac)_2L^R$: a multifrequency EPR study at 34, 122 and 244 GHz

Matvey V. Fedin,[a,1] Sergey L. Veber,[a,c] Galina V. Romanenko,[a] Victor I. Ovcharenko,[a] Renad Z. Sagdeev,[a] Gudrun Klihm,[b] Edward Reijerse,[b] Wolfgang Lubitz,[b] Elena G. Bagryanskaya [a]

[a]*International Tomography Center SB RAS, 630090 Novosibirsk, Russia*

[b]*Max-Planck-Institut für Bioanorganische Chemie, 45470 Mülheim/Ruhr, Germany*

[c]*Novosibirsk State University, 630090 Novosibirsk, Russia*

I. Calculation procedure

The theoretical approach used in the simulations was described in our previous work[1]. Briefly, (i) the multiplets A, B and C of a spin triad are modeled by three paramagnetic centers with the corresponding g-tensors given by eqs.(1); (ii) the intensities of their lines take into account the probabilities of the corresponding EPR transitions and the Boltzman population factors corresponding to the exchange interaction *J*; (iii) the dynamic mixing process between given multiplets M and N is introduced as a reversible monomolecular reaction M↔N with the rate constants coupled by an expression $k_{M\to N} = k_{N\to M}\exp\left(\left(E_M - E_N\right)/kT\right)$, where $E_{M,N}$ are the energies of the corresponding multiplets. The characteristic rate of the mixing (exchange) process is then defined as $k_{MN}^{ex} = k_{M\to N} + k_{N\to M}$, as is usually done for exchange rates. The solution of modified Bloch equations is numerically performed and the arrays of resulting spectra are simultaneously calculated for the three mw bands at certain temperature. The input parameters of the spin triad at certain temperature are: g-factors of the copper ion g^{Cu} and nitroxide g^R, the exchange coupling constant J, the transverse relaxation times $T_2^{A,B,C}$ of each multiplet A, B and C associated with the widths of corresponding lines, and the mixing process rate constants $k_{MN}^{ex} = k_{M\to N} + k_{N\to M}$. The exchange coupling constant is the function of temperature $J = J(T)$ and was estimated by fitting the magnetic susceptibility data $(Cu(hfac)_2L^{Bu}\cdot 0.5C_8H_{10}$ and $Cu(hfac)_2L^{Pr}$, see Section II of

[1] Corresponding author: mfedin@tomo.nsc.ru (M. Fedin)

Supplementary Data) or taken directly as obtained previously by EPR [2] ($Cu(hfac)_2L^{Bu}\cdot 0.5C_8H_{18}$). The g-tensor of the nitroxide was taken isotropic as g^R=2.007. The relaxation times $T_2^{A,B,C}$ influence mainly the linewidth of the signals and were adjusted for each spectrum. The main difficulty in interpretation of the temperature dependence of single crystal EPR of breathing crystals is the fact that the g-tensor of the copper ion also evolves with temperature $\mathbf{g}^{\mathbf{Cu}} = \mathbf{g}^{\mathbf{Cu}}(T)$, and thus the g-value at each temperature has to be adjusted experimentally. Finally, the last variables are the exchange rates between corresponding multiplets k_{MN}^{ex} that of course are constant vs. mw frequency at each particular temperature. This, despite of many variable parameters in simulation, allowed us to obtain rather strict estimates for the mixing rate constants. As was discussed above, we assume that the mixing rates A,B↔C are much slower than A↔B because the former two transitions are weakly allowed due to the anisotropy of exchange coupling. Therefore, following our previous work[1], the mixing rates depend on the energy splitting between corresponding multiplets and temperature according to:

$$k_{MN}^{ex} = K_{MN}\cdot \mathrm{cth}\left(\frac{|E_M - E_N|}{2kT}\right), \qquad \text{(S1)}$$

and $K_{A\leftrightarrow C} \approx K_{B\leftrightarrow C} = \alpha K_{A\leftrightarrow B}$ with $\alpha < 1$ being the measure of exchange anisotropy in the system.

Because there are too many unknown adjustable variables, our focus was to test the agreement of experiment and theory for a reasonable set of parameters and to obtain estimates for the mixing rate constants. We do not generally claim that these sets of parameters (section III of Supplementary Data) are unique, nor do we draw any key conclusions based on the obtained sets. The main purpose of these simulations was to conclude whether it is possible or not to describe the experimental data using the developed approach. An important exception, however, is the case where two resolved lines of a triad are observed at high magnetic field. In this case the simultaneous simulation of EPR spectra at 34, 122 and 244 GHz at certain temperature yields reliable information on the rates of the mixing processes.

II. Estimation of $J(T)$ dependence from the magnetic susceptibility $\mu(T)$

As was mentioned above, the simulations of the EPR spectra require the function $J(T)$. In principle, we have discussed previously[2] the opposite strategy when the $J(T)$ function is obtained from the simulation of single-crystal EPR spectra using the example of complex $Cu(hfac)_2L^{Bu}\cdot 0.5C_8H_{18}$.[2] It should be mentioned, that for a valid evaluation of the $J(T)$ dependence from EPR spectra vs. temperature, two conditions must be fulfilled: (i) the dynamic mixing should be fast (fast exchange limit), and (ii) the proper single crystal orientation has to be chosen, allowing for a constant (or nearly constant) value of g^{Cu} vs. temperature. The first condition is nearly satisfied for $Cu(hfac)_2L^{Pr}$ at Q-band, but is hardly satisfied for $Cu(hfac)_2L^{Bu}\cdot 0.5C_8H_{10}$ even at Q-band meaning that the lower frequency band has to be chosen for this kind of study. The second condition was difficult to fulfill due to experimental complications at high field. Therefore, in the present work we do not aim at precise finding $J(T)$ functions using EPR (which will be the topic of a forthcoming publication[3]), but estimate $J(T)$ for $Cu(hfac)_2L^{Pr}$ and $Cu(hfac)_2L^{Bu}\cdot 0.5C_8H_{10}$ from magnetic susceptibility data. As was discussed previously[4], the magnetic susceptibility dependence can be simulated using the expression:

$$\mu_{\text{eff}}^2 = 0.5\mu_{\text{tr,eff}}^2 + 0.5\mu_{\text{is,eff}}^2 = \frac{3\left(g^{\text{A}}\right)^2 + 3\left(g^{\text{B}}\right)^2 \cdot e^{2J/kT} + 30\left(g^{\text{C}}\right)^2 \cdot e^{3J/kT}}{8\left(1 + e^{2J/kT} + 2e^{3J/kT}\right)} + 0.5\mu_{\text{is,eff}}^2, \qquad \text{(S2)}$$

where subscripts "tr" and "is" correspond to the spin triad and isolated copper ion, respectively. The exchange interaction between a triad and an isolated copper (inter-cluster exchange) significantly influences the magnetic susceptibility curves at low temperatures (typically <20 K) only. Thus, for simple estimations one can neglect this inter-cluster exchange interaction at higher temperatures and use the temperature-independent value $\mu_{\text{is,eff}} \approx 1.86\ \beta$ which corresponds to the uncoupled spin S=1/2 of copper with average $g\approx 2.15$. g^A, g^B and g^C are functions of g^R=2.007 and g^{Cu} given by equations (1), where again the g-factor of copper was estimated as $g^{Cu} \approx 2.15$ (average value is justified for the disordered powder measurement in the magnetic susceptibility experiment).

Estimation for $Cu(hfac)_2L^{Pr}$

T / K	J / cm^{-1}
59.9500	-120.4721
79.8500	-113.7138
100.2900	-105.7733
120.5500	-99.9223
140.2736	-96.8042
159.8133	-89.8682
180.0500	-80.5158
199.8300	-68.7186
211.5400	-59.8721
215.1700	-56.3763
220.3500	-49.5961
223.0100	-41.1150
226.0800	-36.9315
228.8700	-32.5317
231.9000	-28.3620
234.8000	-24.4170
237.7600	-20.7361
240.7300	-17.3606
260.9700	-8.5144
301.2100	-1.0772

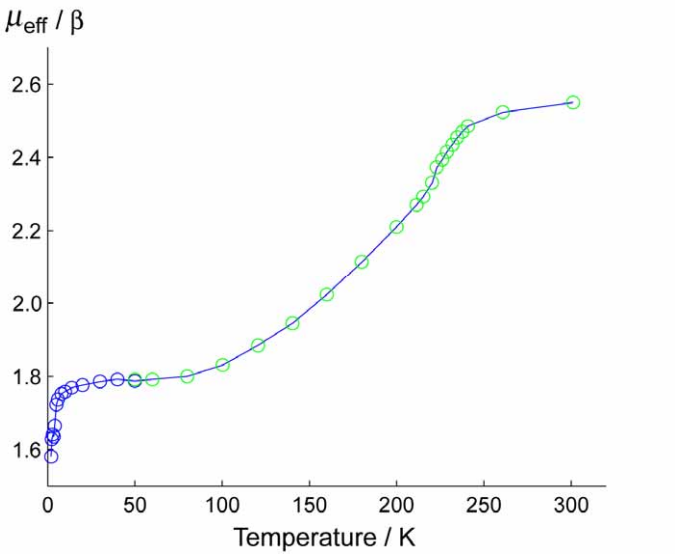

Figure S1. Experimental dependence $\mu_{eff}(T)$ of $Cu(hfac)_2L^{Pr}$ (blue) and the fit using eq.(S2) and $J(T)$ dependence given in the table (green).

Estimation for $Cu(hfac)_2L^{Bu}\cdot 0.5C_8H_{10}$

T / K	J / cm^{-1}
80.3400	-92.8210
90.5200	-92.8210
100.5500	-92.8317
110.5700	-93.0340
120.5300	-89.8457
130.4300	-86.0508
140.3000	-81.1983
150.3500	-75.6603
159.5800	-71.2009
169.5400	-66.2830
179.5200	-61.9884
189.5500	-57.7528
199.5500	-53.4641
209.6400	-49.2734
219.7500	-44.8598
229.8900	-41.0846
239.8500	-37.7786
249.9200	-34.4466
259.9100	-31.5866
269.9300	-28.8725
279.9200	-26.4766
290.0300	-23.7327
300.0400	-21.8176

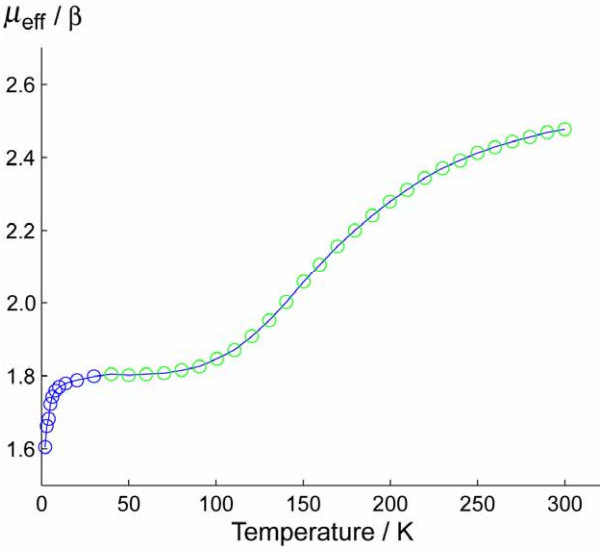

Figure S2. Experimental dependence $\mu_{eff}(T)$ of $Cu(hfac)_2L^{Bu}\cdot 0.5C_8H_{10}$ (blue) and the fit using eq.(S2) and $J(T)$ dependence given in the table (green).

III. Parameters used in simulations

Input parameters T, J, g^{L}, g^{Cu}, T_2^A, T_2^B, T_2^C, K, α and the calculated rates of dynamic mixing processes $k^{ex}_{A\leftrightarrow B}$, $k^{ex}_{A\leftrightarrow C}$ and $k^{ex}_{B\leftrightarrow C}$ are listed for each compound and each frequency band. The calculated spectra using given sets of parameters are shown in figures 3-5.

(1) Parameters used in simulation of EPR spectra of breathing crystal $Cu(hfac)_2L^{Pr}$

$\nu_{mw}\approx33.97$ GHz

T / K	J / cm^{-1}	g^{L}	g^{Cu}	T_2^A / s	T_2^B / s	T_2^C / s	K / s^{-1}	α	$k^{ex}_{A\leftrightarrow B}$ / s^{-1}	$k^{ex}_{A\leftrightarrow C}$ / s^{-1}	$k^{ex}_{B\leftrightarrow C}$ / s^{-1}
90	-110	2.007	2.11	$1\cdot10^{-9}$	$8\cdot10^{-10}$	$4\cdot10^{-10}$	$2\cdot10^{10}$	$6\cdot10^{-2}$	$2.12\cdot10^{10}$	$1.21\cdot10^{9}$	$1.69\cdot10^{9}$
110	-103	2.007	2.11	$8\cdot10^{-10}$	$8\cdot10^{-10}$	$4\cdot10^{-10}$	$2\cdot10^{10}$	$6\cdot10^{-2}$	$2.28\cdot10^{10}$	$1.24\cdot10^{9}$	$2.04\cdot10^{9}$
130	-98	2.007	2.11	$8\cdot10^{-10}$	$8\cdot10^{-10}$	$3\cdot10^{-10}$	$4\cdot10^{10}$	$6\cdot10^{-2}$	$5.03\cdot10^{10}$	$2.59\cdot10^{9}$	$4.85\cdot10^{9}$
140	-96	2.007	2.11	$8\cdot10^{-10}$	$8\cdot10^{-10}$	$3\cdot10^{-10}$	$4\cdot10^{10}$	$6\cdot10^{-2}$	$5.29\cdot10^{10}$	$2.66\cdot10^{9}$	$5.25\cdot10^{9}$
150	-93	2.007	2.11	$8\cdot10^{-10}$	$8\cdot10^{-10}$	$3\cdot10^{-10}$	$4.5\cdot10^{10}$	$6\cdot10^{-2}$	$6.39\cdot10^{10}$	$3.12\cdot10^{9}$	$6.56\cdot10^{9}$
160	-89	2.007	2.12	$8\cdot10^{-10}$	$8\cdot10^{-10}$	$3\cdot10^{-10}$	$5\cdot10^{10}$	$6\cdot10^{-2}$	$7.59\cdot10^{10}$	$3.61\cdot10^{9}$	$7.98\cdot10^{9}$
170	-84	2.007	2.14	$8\cdot10^{-10}$	$8\cdot10^{-10}$	$3\cdot10^{-10}$	$5.5\cdot10^{10}$	$6\cdot10^{-2}$	$8.99\cdot10^{10}$	$4.18\cdot10^{9}$	$9.67\cdot10^{9}$
180	-80	2.007	2.15	$8\cdot10^{-10}$	$8\cdot10^{-10}$	$3\cdot10^{-10}$	$7\cdot10^{10}$	$6\cdot10^{-2}$	$1.24\cdot10^{10}$	$5.64\cdot10^{9}$	$1.35\cdot10^{10}$
200	-68	2.007	2.16	$8\cdot10^{-10}$	$8\cdot10^{-10}$	$2.5\cdot10^{-10}$	$6\cdot10^{10}$	$6\cdot10^{-2}$	$1.32\cdot10^{11}$	$5.75\cdot10^{9}$	$1.50\cdot10^{10}$
215	-56	2.007	2.17	$8\cdot10^{-10}$	$8\cdot10^{-10}$	$2\cdot10^{-10}$	$10\cdot10^{10}$	$6\cdot10^{-2}$	$2.79\cdot10^{11}$	$1.17\cdot10^{10}$	$3.23\cdot10^{10}$
250	-10	2.007	2.18	$8\cdot10^{-10}$	$8\cdot10^{-10}$	$2\cdot10^{-10}$	$12\cdot10^{10}$	$6\cdot10^{-2}$	$2.08\cdot10^{12}$	$8.36\cdot10^{10}$	$2.50\cdot10^{11}$

$\nu_{mw}\approx121.46$ GHz

T / K	J / cm^{-1}	g^{L}	g^{Cu}	T_2^A / s	T_2^B / s	T_2^C / s	K / s^{-1}	α	$k^{ex}_{A\leftrightarrow B}$ / s^{-1}	$k^{ex}_{A\leftrightarrow C}$ / s^{-1}	$k^{ex}_{B\leftrightarrow C}$ / s^{-1}
90	-110	2.007	2.138	$1.5\cdot10^{-9}$	$2\cdot10^{-10}$	$1\cdot10^{-10}$	$2\cdot10^{10}$	$6\cdot10^{-2}$	$2.12\cdot10^{10}$	$1.21\cdot10^{9}$	$1.69\cdot10^{9}$
110	-103	2.007	2.138	$8\cdot10^{-10}$	$2\cdot10^{-10}$	$1\cdot10^{-10}$	$2\cdot10^{10}$	$6\cdot10^{-2}$	$2.28\cdot10^{10}$	$1.24\cdot10^{9}$	$2.04\cdot10^{9}$
130	-98	2.007	2.138	$8\cdot10^{-10}$	$2\cdot10^{-10}$	$1\cdot10^{-10}$	$4\cdot10^{10}$	$6\cdot10^{-2}$	$5.03\cdot10^{10}$	$2.59\cdot10^{9}$	$4.85\cdot10^{9}$
140	-96	2.007	2.138	$8\cdot10^{-10}$	$2\cdot10^{-10}$	$1\cdot10^{-10}$	$4\cdot10^{10}$	$6\cdot10^{-2}$	$5.29\cdot10^{10}$	$2.66\cdot10^{9}$	$5.25\cdot10^{9}$
150	-93	2.007	2.138	$3\cdot10^{-10}$	$2\cdot10^{-10}$	$1\cdot10^{-10}$	$4.5\cdot10^{10}$	$6\cdot10^{-2}$	$6.39\cdot10^{10}$	$3.12\cdot10^{9}$	$6.56\cdot10^{9}$
160	-89	2.007	2.138	$3\cdot10^{-10}$	$2\cdot10^{-10}$	$1\cdot10^{-10}$	$5\cdot10^{10}$	$6\cdot10^{-2}$	$7.59\cdot10^{10}$	$3.61\cdot10^{9}$	$7.98\cdot10^{9}$
170	-84	2.007	2.138	$3\cdot10^{-10}$	$2\cdot10^{-10}$	$1\cdot10^{-10}$	$5.5\cdot10^{10}$	$6\cdot10^{-2}$	$8.99\cdot10^{10}$	$4.18\cdot10^{9}$	$9.67\cdot10^{9}$
180	-80	2.007	2.138	$3\cdot10^{-10}$	$2\cdot10^{-10}$	$1\cdot10^{-10}$	$7\cdot10^{10}$	$6\cdot10^{-2}$	$1.24\cdot10^{10}$	$5.64\cdot10^{9}$	$1.35\cdot10^{10}$
200	-68	2.007	2.138	$3\cdot10^{-10}$	$2\cdot10^{-10}$	$1\cdot10^{-10}$	$6\cdot10^{10}$	$6\cdot10^{-2}$	$1.32\cdot10^{11}$	$5.75\cdot10^{9}$	$1.50\cdot10^{10}$
215	-56	2.007	2.138	$3\cdot10^{-10}$	$2\cdot10^{-10}$	$1.2\cdot10^{-10}$	$10\cdot10^{10}$	$6\cdot10^{-2}$	$2.79\cdot10^{11}$	$1.17\cdot10^{10}$	$3.23\cdot10^{10}$
260	-10	2.007	2.160	$3\cdot10^{-10}$	$2\cdot10^{-10}$	$1.7\cdot10^{-10}$	$12\cdot10^{10}$	$6\cdot10^{-2}$	$2.50\cdot10^{13}$	$1.00\cdot10^{12}$	$3.00\cdot10^{12}$

$\nu_{mw}\approx243.10$ GHz

T / K	J / cm^{-1}	g^{L}	g^{Cu}	T_2^A / s	T_2^B / s	T_2^C / s	K / s^{-1}	α	$k^{ex}_{A\leftrightarrow B}$ / s^{-1}	$k^{ex}_{A\leftrightarrow C}$ / s^{-1}	$k^{ex}_{B\leftrightarrow C}$ / s^{-1}
90	-110	2.007	2.135	$5\cdot10^{-10}$	$2\cdot10^{-10}$	$1\cdot10^{-10}$	$2\cdot10^{10}$	$6\cdot10^{-2}$	$2.12\cdot10^{10}$	$1.21\cdot10^{9}$	$1.69\cdot10^{9}$
110	-103	2.007	2.135	$5\cdot10^{-10}$	$2\cdot10^{-10}$	$1\cdot10^{-10}$	$2\cdot10^{10}$	$6\cdot10^{-2}$	$2.28\cdot10^{10}$	$1.24\cdot10^{9}$	$2.04\cdot10^{9}$
130	-98	2.007	2.135	$5\cdot10^{-10}$	$2\cdot10^{-10}$	$1\cdot10^{-10}$	$4\cdot10^{10}$	$6\cdot10^{-2}$	$5.03\cdot10^{10}$	$2.59\cdot10^{9}$	$4.85\cdot10^{9}$
140	-96	2.007	2.135	$5\cdot10^{-10}$	$2\cdot10^{-10}$	$1\cdot10^{-10}$	$4\cdot10^{10}$	$6\cdot10^{-2}$	$5.29\cdot10^{10}$	$2.66\cdot10^{9}$	$5.25\cdot10^{9}$
150	-93	2.007	2.135	$5\cdot10^{-10}$	$2\cdot10^{-10}$	$1\cdot10^{-10}$	$4.5\cdot10^{10}$	$6\cdot10^{-2}$	$6.39\cdot10^{10}$	$3.12\cdot10^{9}$	$6.56\cdot10^{9}$
160	-89	2.007	2.135	$3\cdot10^{-10}$	$2\cdot10^{-10}$	$1\cdot10^{-10}$	$5\cdot10^{10}$	$6\cdot10^{-2}$	$7.59\cdot10^{10}$	$3.61\cdot10^{9}$	$7.98\cdot10^{9}$
170	-84	2.007	2.135	$3\cdot10^{-10}$	$2\cdot10^{-10}$	$1\cdot10^{-10}$	$5.5\cdot10^{10}$	$6\cdot10^{-2}$	$8.99\cdot10^{10}$	$4.18\cdot10^{9}$	$9.67\cdot10^{9}$
180	-80	2.007	2.135	$3\cdot10^{-10}$	$2\cdot10^{-10}$	$1\cdot10^{-10}$	$7\cdot10^{10}$	$6\cdot10^{-2}$	$1.24\cdot10^{10}$	$5.64\cdot10^{9}$	$1.35\cdot10^{10}$
200	-68	2.007	2.147	$3\cdot10^{-10}$	$2\cdot10^{-10}$	$9\cdot10^{-11}$	$6\cdot10^{10}$	$6\cdot10^{-2}$	$1.32\cdot10^{11}$	$5.75\cdot10^{9}$	$1.50\cdot10^{10}$
215	-56	2.007	2.150	$3\cdot10^{-10}$	$2\cdot10^{-10}$	$6\cdot10^{-11}$	$10\cdot10^{10}$	$6\cdot10^{-2}$	$2.79\cdot10^{11}$	$1.17\cdot10^{10}$	$3.23\cdot10^{10}$
250	-10	2.007	2.160	$3\cdot10^{-10}$	$2\cdot10^{-10}$	$9\cdot10^{-11}$	$12\cdot10^{10}$	$6\cdot10^{-2}$	$2.71\cdot10^{12}$	$1.08\cdot10^{11}$	$3.25\cdot10^{11}$

(2) Parameters used in simulation of EPR spectra of breathing crystal $Cu(hfac)_2L^{Bu}\cdot 0.5C_8H_{10}$

$\nu_{mw}\approx 33.97$ GHz

T / K	J / cm^{-1}	g^L	g^{Cu}	T_2^A / s	T_2^B / s	T_2^C / s	K / s^{-1}	α	$k^{ex}_{A\leftrightarrow B}$ / s^{-1}	$k^{ex}_{A\leftrightarrow C}$ / s^{-1}	$k^{ex}_{B\leftrightarrow C}$ / s^{-1}
70	-92	2.007	2.25	$5\cdot10^{-10}$	$5\cdot10^{-10}$	$4\cdot10^{-10}$	$2\cdot10^{10}$	$6\cdot10^{-2}$	$2.09\cdot10^{10}$	$1.20\cdot10^{9}$	$1.62\cdot10^{9}$
90	-92	2.007	2.25	$5\cdot10^{-10}$	$5\cdot10^{-10}$	$2\cdot10^{-10}$	$2.5\cdot10^{10}$	$6\cdot10^{-2}$	$2.77\cdot10^{10}$	$1.53\cdot10^{9}$	$2.39\cdot10^{9}$
110	-92	2.007	2.24	$5\cdot10^{-10}$	$5\cdot10^{-10}$	$1\cdot10^{-10}$	$3\cdot10^{10}$	$6\cdot10^{-2}$	$3.59\cdot10^{10}$	$1.90\cdot10^{9}$	$3.34\cdot10^{9}$
170	-66	2.007	2.09	$9\cdot10^{-10}$	$7\cdot10^{-10}$	$2\cdot10^{-10}$	$4\cdot10^{10}$	$6\cdot10^{-2}$	$7.89\cdot10^{10}$	$3.50\cdot10^{9}$	$8.81\cdot10^{9}$
180	-61	2.007	2.09	$9\cdot10^{-10}$	$7\cdot10^{-10}$	$2\cdot10^{-10}$	$4\cdot10^{10}$	$6\cdot10^{-2}$	$8.84\cdot10^{10}$	$3.84\cdot10^{9}$	$1.00\cdot10^{10}$
200	-53	2.007	2.11	$9\cdot10^{-10}$	$7\cdot10^{-10}$	$2\cdot10^{-10}$	$4\cdot10^{10}$	$6\cdot10^{-2}$	$1.09\cdot10^{11}$	$4.64\cdot10^{9}$	$1.27\cdot10^{10}$
250	-34	2.007	2.11	$9\cdot10^{-10}$	$7\cdot10^{-10}$	$2\cdot10^{-10}$	$4\cdot10^{10}$	$6\cdot10^{-2}$	$2.07\cdot10^{11}$	$8.41\cdot10^{9}$	$2.46\cdot10^{10}$

$\nu_{mw}\approx 121.48$ GHz

T / K	J / cm^{-1}	g^L	g^{Cu}	T_2^A / s	T_2^B / s	T_2^C / s	K / s^{-1}	α	$k^{ex}_{A\leftrightarrow B}$ / s^{-1}	$k^{ex}_{A\leftrightarrow C}$ / s^{-1}	$k^{ex}_{B\leftrightarrow C}$ / s^{-1}
70	-92	2.007	2.22	$8\cdot10^{-10}$	$2\cdot10^{-10}$	$1\cdot10^{-10}$	$2\cdot10^{10}$	$6\cdot10^{-2}$	$2.09\cdot10^{10}$	$1.20\cdot10^{9}$	$1.62\cdot10^{9}$
90	-92	2.007	2.22	$8\cdot10^{-10}$	$2\cdot10^{-10}$	$1\cdot10^{-10}$	$2.5\cdot10^{10}$	$6\cdot10^{-2}$	$2.77\cdot10^{10}$	$1.53\cdot10^{9}$	$2.39\cdot10^{9}$
110	-92	2.007	2.22	$8\cdot10^{-10}$	$2\cdot10^{-10}$	$1\cdot10^{-10}$	$3\cdot10^{10}$	$6\cdot10^{-2}$	$3.59\cdot10^{10}$	$1.90\cdot10^{9}$	$3.34\cdot10^{9}$
170	-66	2.007	2.11	$8\cdot10^{-10}$	$3\cdot10^{-10}$	$2\cdot10^{-10}$	$4\cdot10^{10}$	$6\cdot10^{-2}$	$7.89\cdot10^{10}$	$3.50\cdot10^{9}$	$8.81\cdot10^{9}$
180	-61	2.007	2.11	$8\cdot10^{-10}$	$3\cdot10^{-10}$	$2\cdot10^{-10}$	$4\cdot10^{10}$	$6\cdot10^{-2}$	$8.84\cdot10^{10}$	$3.84\cdot10^{9}$	$1.00\cdot10^{10}$
200	-53	2.007	2.14	$8\cdot10^{-10}$	$3\cdot10^{-10}$	$2\cdot10^{-10}$	$4\cdot10^{10}$	$6\cdot10^{-2}$	$1.09\cdot10^{11}$	$4.64\cdot10^{9}$	$1.27\cdot10^{10}$
220	-44	2.007	2.14	$8\cdot10^{-10}$	$3\cdot10^{-10}$	$2\cdot10^{-10}$	$4\cdot10^{10}$	$6\cdot10^{-2}$	$1.42\cdot10^{11}$	$5.90\cdot10^{9}$	$1.67\cdot10^{10}$
260	-31	2.007	2.15	$8\cdot10^{-10}$	$3\cdot10^{-10}$	$2\cdot10^{-10}$	$4\cdot10^{10}$	$6\cdot10^{-2}$	$2.35\cdot10^{11}$	$9.53\cdot10^{9}$	$2.80\cdot10^{10}$

$\nu_{mw}\approx 243.07$ GHz

T / K	J / cm^{-1}	g^L	g^{Cu}	T_2^A / s	T_2^B / s	T_2^C / s	K / s^{-1}	α	$k^{ex}_{A\leftrightarrow B}$ / s^{-1}	$k^{ex}_{A\leftrightarrow C}$ / s^{-1}	$k^{ex}_{B\leftrightarrow C}$ / s^{-1}
70	-92	2.007	2.245	$5\cdot10^{-10}$	$2\cdot10^{-10}$	$1\cdot10^{-10}$	$2\cdot10^{10}$	$6\cdot10^{-2}$	$2.09\cdot10^{10}$	$1.20\cdot10^{9}$	$1.62\cdot10^{9}$
90	-92	2.007	2.245	$5\cdot10^{-10}$	$2\cdot10^{-10}$	$1\cdot10^{-10}$	$2.5\cdot10^{10}$	$6\cdot10^{-2}$	$2.77\cdot10^{10}$	$1.53\cdot10^{9}$	$2.39\cdot10^{9}$
110	-92	2.007	2.245	$5\cdot10^{-10}$	$2\cdot10^{-10}$	$5\cdot10^{-11}$	$3\cdot10^{10}$	$6\cdot10^{-2}$	$3.59\cdot10^{10}$	$1.90\cdot10^{9}$	$3.34\cdot10^{9}$
120	-90	2.007	2.245	$5\cdot10^{-10}$	$2\cdot10^{-10}$	$5\cdot10^{-11}$	$3\cdot10^{10}$	$6\cdot10^{-2}$	$3.78\cdot10^{10}$	$1.94\cdot10^{9}$	$3.65\cdot10^{9}$
130	-86	2.007	2.245	$5\cdot10^{-10}$	$2\cdot10^{-10}$	$1\cdot10^{-10}$	$4\cdot10^{10}$	$6\cdot10^{-2}$	$5.40\cdot10^{10}$	$2.69\cdot10^{9}$	$5.41\cdot10^{9}$
140	-81	2.007	2.245	$5\cdot10^{-10}$	$2\cdot10^{-10}$	$2\cdot10^{-10}$	$4\cdot10^{10}$	$6\cdot10^{-2}$	$5.86\cdot10^{10}$	$2.83\cdot10^{9}$	$6.09\cdot10^{9}$
150	-75	2.007	2.245	$5\cdot10^{-10}$	$2\cdot10^{-10}$	$2\cdot10^{-10}$	$4\cdot10^{10}$	$6\cdot10^{-2}$	$6.48\cdot10^{10}$	$3.02\cdot10^{9}$	$6.95\cdot10^{9}$
160	-71	2.007	2.070	$5\cdot10^{-10}$	$2\cdot10^{-10}$	$1\cdot10^{-10}$	$4\cdot10^{10}$	$6\cdot10^{-2}$	$7.09\cdot10^{10}$	$3.22\cdot10^{9}$	$7.77\cdot10^{9}$
180	-61	2.007	2.070	$5\cdot10^{-10}$	$2\cdot10^{-10}$	$1\cdot10^{-10}$	$4\cdot10^{10}$	$6\cdot10^{-2}$	$8.84\cdot10^{10}$	$3.84\cdot10^{9}$	$1.00\cdot10^{10}$
220	-44	2.007	2.105	$5\cdot10^{-10}$	$2\cdot10^{-10}$	$1\cdot10^{-10}$	$4\cdot10^{10}$	$6\cdot10^{-2}$	$1.42\cdot10^{11}$	$5.90\cdot10^{9}$	$1.67\cdot10^{10}$
260	-31	2.007	2.128	$5\cdot10^{-10}$	$2\cdot10^{-10}$	$1\cdot10^{-10}$	$4\cdot10^{10}$	$6\cdot10^{-2}$	$2.35\cdot10^{11}$	$9.53\cdot10^{9}$	$2.80\cdot10^{10}$

(3) Parameters used in simulation of EPR spectra of breathing crystal $Cu(hfac)_2L^{Bu}\cdot 0.5C_8H_{18}$

$\nu_{mw}\approx 33.96$ GHz

T / K	J / cm^{-1}	g^L	g^{Cu}	T_2^A / s	T_2^B / s	T_2^C / s	K / s^{-1}	α	$k^{ex}_{A\leftrightarrow B}$ / s^{-1}	$k^{ex}_{A\leftrightarrow C}$ / s^{-1}	$k^{ex}_{B\leftrightarrow C}$ / s^{-1}
50	-140	2.007	2.074	$4\cdot10^{-9}$	$4\cdot10^{-9}$	$3\cdot10^{-10}$	$2\cdot10^{11}$	$6\cdot10^{-2}$	$2.00\cdot10^{11}$	$1.20\cdot10^{10}$	$1.24\cdot10^{10}$
70	-120	2.007	2.074	$4\cdot10^{-9}$	$4\cdot10^{-9}$	$3\cdot10^{-10}$	$2\cdot10^{11}$	$6\cdot10^{-2}$	$2.02\cdot10^{11}$	$1.20\cdot10^{10}$	$1.42\cdot10^{10}$
90	-100	2.007	2.075	$4\cdot10^{-9}$	$4\cdot10^{-9}$	$3\cdot10^{-10}$	$2\cdot10^{11}$	$6\cdot10^{-2}$	$2.17\cdot10^{11}$	$1.22\cdot10^{10}$	$1.80\cdot10^{10}$
100	-90	2.007	2.075	$4\cdot10^{-9}$	$4\cdot10^{-9}$	$3\cdot10^{-10}$	$2\cdot10^{11}$	$6\cdot10^{-2}$	$2.32\cdot10^{11}$	$1.25\cdot10^{10}$	$2.10\cdot10^{10}$
110	-75	2.007	2.075	$4\cdot10^{-9}$	$4\cdot10^{-9}$	$3\cdot10^{-10}$	$3\cdot10^{11}$	$6\cdot10^{-2}$	$4.08\cdot10^{11}$	$2.02\cdot10^{10}$	$4.11\cdot10^{10}$
120	-70	2.007	2.190	$4\cdot10^{-9}$	$4\cdot10^{-9}$	$3\cdot10^{-10}$	$4\cdot10^{11}$	$6\cdot10^{-2}$	$5.83\cdot10^{11}$	$2.82\cdot10^{10}$	$6.05\cdot10^{10}$
130	-60	2.007	2.170	$4\cdot10^{-9}$	$4\cdot10^{-9}$	$3\cdot10^{-10}$	$4\cdot10^{11}$	$6\cdot10^{-2}$	$6.88\cdot10^{11}$	$3.15\cdot10^{10}$	$7.49\cdot10^{10}$
140	-51	2.007	2.160	$4\cdot10^{-9}$	$4\cdot10^{-9}$	$3\cdot10^{-10}$	$4\cdot10^{11}$	$6\cdot10^{-2}$	$8.31\cdot10^{11}$	$3.65\cdot10^{10}$	$9.36\cdot10^{10}$
150	-38	2.007	2.160	$4\cdot10^{-9}$	$4\cdot10^{-9}$	$3\cdot10^{-10}$	$4\cdot10^{11}$	$6\cdot10^{-2}$	$1.14\cdot10^{12}$	$4.81\cdot10^{10}$	$1.33\cdot10^{11}$
160	-25	2.007	2.160	$4\cdot10^{-9}$	$4\cdot10^{-9}$	$3\cdot10^{-10}$	$4\cdot10^{11}$	$6\cdot10^{-2}$	$1.80\cdot10^{12}$	$7.38\cdot10^{10}$	$2.14\cdot10^{11}$
170	-16	2.007	2.160	$4\cdot10^{-9}$	$4\cdot10^{-9}$	$3\cdot10^{-10}$	$4\cdot10^{11}$	$6\cdot10^{-2}$	$2.97\cdot10^{12}$	$1.19\cdot10^{11}$	$3.55\cdot10^{11}$
180	-7	2.007	2.160	$4\cdot10^{-9}$	$4\cdot10^{-9}$	$3\cdot10^{-10}$	$4\cdot10^{11}$	$6\cdot10^{-2}$	$7.15\cdot10^{12}$	$2.86\cdot10^{11}$	$8.58\cdot10^{11}$
200	-5	2.007	2.150	$4\cdot10^{-9}$	$4\cdot10^{-9}$	$3\cdot10^{-10}$	$4\cdot10^{11}$	$6\cdot10^{-2}$	$1.11\cdot10^{13}$	$4.45\cdot10^{11}$	$1.33\cdot10^{12}$
220	-5	2.007	2.147	$4\cdot10^{-9}$	$4\cdot10^{-9}$	$3\cdot10^{-10}$	$4\cdot10^{11}$	$6\cdot10^{-2}$	$1.22\cdot10^{13}$	$4.89\cdot10^{11}$	$1.46\cdot10^{12}$

$\nu_{mw}\approx 122.00$ GHz

T / K	J / cm^{-1}	g^L	g^{Cu}	T_2^A / s	T_2^B / s	T_2^C / s	K / s^{-1}	α	$k^{ex}_{A\leftrightarrow B}$ / s^{-1}	$k^{ex}_{A\leftrightarrow C}$ / s^{-1}	$k^{ex}_{B\leftrightarrow C}$ / s^{-1}
50	-140	2.007	2.080	$2\cdot10^{-9}$	$2\cdot10^{-9}$	$4.5\cdot10^{-10}$	$2\cdot10^{11}$	$6\cdot10^{-2}$	$2.00\cdot10^{11}$	$1.20\cdot10^{10}$	$1.24\cdot10^{10}$
70	-120	2.007	2.090	$2\cdot10^{-9}$	$2\cdot10^{-9}$	$4.5\cdot10^{-10}$	$2\cdot10^{11}$	$6\cdot10^{-2}$	$2.02\cdot10^{11}$	$1.20\cdot10^{10}$	$1.42\cdot10^{10}$
90	-100	2.007	2.102	$2\cdot10^{-9}$	$2\cdot10^{-9}$	$4.5\cdot10^{-10}$	$2\cdot10^{11}$	$6\cdot10^{-2}$	$2.17\cdot10^{11}$	$1.22\cdot10^{10}$	$1.80\cdot10^{10}$
100	-90	2.007	2.110	$2\cdot10^{-9}$	$2\cdot10^{-9}$	$4.5\cdot10^{-10}$	$2\cdot10^{11}$	$6\cdot10^{-2}$	$2.32\cdot10^{11}$	$1.25\cdot10^{10}$	$2.10\cdot10^{10}$
110	-75	2.007	2.110	$2\cdot10^{-9}$	$2\cdot10^{-9}$	$4.5\cdot10^{-10}$	$3\cdot10^{11}$	$6\cdot10^{-2}$	$4.08\cdot10^{11}$	$2.02\cdot10^{10}$	$4.11\cdot10^{10}$
120	-70	2.007	2.110	$2\cdot10^{-9}$	$2\cdot10^{-9}$	$4.5\cdot10^{-10}$	$4\cdot10^{11}$	$6\cdot10^{-2}$	$5.83\cdot10^{11}$	$2.82\cdot10^{10}$	$6.05\cdot10^{10}$
130	-60	2.007	2.100	$2\cdot10^{-9}$	$2\cdot10^{-9}$	$4.5\cdot10^{-10}$	$4\cdot10^{11}$	$6\cdot10^{-2}$	$6.88\cdot10^{11}$	$3.15\cdot10^{10}$	$7.49\cdot10^{10}$
140	-51	2.007	2.110	$2\cdot10^{-9}$	$2\cdot10^{-9}$	$4.5\cdot10^{-10}$	$4\cdot10^{11}$	$6\cdot10^{-2}$	$8.31\cdot10^{11}$	$3.65\cdot10^{10}$	$9.36\cdot10^{10}$
150	-38	2.007	2.115	$2\cdot10^{-9}$	$2\cdot10^{-9}$	$4.5\cdot10^{-10}$	$4\cdot10^{11}$	$6\cdot10^{-2}$	$1.14\cdot10^{12}$	$4.81\cdot10^{10}$	$1.33\cdot10^{11}$
160	-25	2.007	2.125	$2\cdot10^{-9}$	$2\cdot10^{-9}$	$4.5\cdot10^{-10}$	$4\cdot10^{11}$	$6\cdot10^{-2}$	$1.80\cdot10^{12}$	$7.38\cdot10^{10}$	$2.14\cdot10^{11}$
170	-16	2.007	2.125	$2\cdot10^{-9}$	$2\cdot10^{-9}$	$4.5\cdot10^{-10}$	$4\cdot10^{11}$	$6\cdot10^{-2}$	$2.97\cdot10^{12}$	$1.19\cdot10^{11}$	$3.55\cdot10^{11}$
180	-7	2.007	2.125	$2\cdot10^{-9}$	$2\cdot10^{-9}$	$4.5\cdot10^{-10}$	$4\cdot10^{11}$	$6\cdot10^{-2}$	$7.15\cdot10^{12}$	$2.86\cdot10^{11}$	$8.58\cdot10^{11}$
200	-5	2.007	2.128	$2\cdot10^{-9}$	$2\cdot10^{-9}$	$4.5\cdot10^{-10}$	$4\cdot10^{11}$	$6\cdot10^{-2}$	$1.11\cdot10^{13}$	$4.45\cdot10^{11}$	$1.33\cdot10^{12}$
220	-5	2.007	2.130	$2\cdot10^{-9}$	$2\cdot10^{-9}$	$4.5\cdot10^{-10}$	$4\cdot10^{11}$	$6\cdot10^{-2}$	$1.22\cdot10^{13}$	$4.89\cdot10^{11}$	$1.46\cdot10^{12}$

$\nu_{mw}\approx 243.80$ GHz

T / K	J / cm^{-1}	g^L	g^{Cu}	T_2^A / s	T_2^B / s	T_2^C / s	K / s^{-1}	α	$k^{ex}_{A\leftrightarrow B}$ / s^{-1}	$k^{ex}_{A\leftrightarrow C}$ / s^{-1}	$k^{ex}_{B\leftrightarrow C}$ / s^{-1}
50	-140	2.007	2.085	$1\cdot10^{-9}$	$1\cdot10^{-9}$	$3.5\cdot10^{-10}$	$2\cdot10^{11}$	$6\cdot10^{-2}$	$2.00\cdot10^{11}$	$1.20\cdot10^{10}$	$1.24\cdot10^{10}$
70	-120	2.007	2.092	$1\cdot10^{-9}$	$1\cdot10^{-9}$	$3.5\cdot10^{-10}$	$2\cdot10^{11}$	$6\cdot10^{-2}$	$2.02\cdot10^{11}$	$1.20\cdot10^{10}$	$1.42\cdot10^{10}$
90	-100	2.007	2.103	$1\cdot10^{-9}$	$1\cdot10^{-9}$	$3.5\cdot10^{-10}$	$2\cdot10^{11}$	$6\cdot10^{-2}$	$2.17\cdot10^{11}$	$1.22\cdot10^{10}$	$1.80\cdot10^{10}$
100	-90	2.007	2.103	$1\cdot10^{-9}$	$1\cdot10^{-9}$	$3.5\cdot10^{-10}$	$2\cdot10^{11}$	$6\cdot10^{-2}$	$2.32\cdot10^{11}$	$1.25\cdot10^{10}$	$2.10\cdot10^{10}$
110	-75	2.007	2.110	$1\cdot10^{-9}$	$1\cdot10^{-9}$	$3.5\cdot10^{-10}$	$3\cdot10^{11}$	$6\cdot10^{-2}$	$4.08\cdot10^{11}$	$2.02\cdot10^{10}$	$4.11\cdot10^{10}$
120	-70	2.007	2.110	$1\cdot10^{-9}$	$1\cdot10^{-9}$	$3.5\cdot10^{-10}$	$4\cdot10^{11}$	$6\cdot10^{-2}$	$5.83\cdot10^{11}$	$2.82\cdot10^{10}$	$6.05\cdot10^{10}$
130	-60	2.007	2.110	$1\cdot10^{-9}$	$1\cdot10^{-9}$	$3.5\cdot10^{-10}$	$4\cdot10^{11}$	$6\cdot10^{-2}$	$6.88\cdot10^{11}$	$3.15\cdot10^{10}$	$7.49\cdot10^{10}$
140	-51	2.007	2.120	$1\cdot10^{-9}$	$1\cdot10^{-9}$	$3.5\cdot10^{-10}$	$4\cdot10^{11}$	$6\cdot10^{-2}$	$8.31\cdot10^{11}$	$3.65\cdot10^{10}$	$9.36\cdot10^{10}$
150	-38	2.007	2.130	$1\cdot10^{-9}$	$1\cdot10^{-9}$	$3.5\cdot10^{-10}$	$4\cdot10^{11}$	$6\cdot10^{-2}$	$1.14\cdot10^{12}$	$4.81\cdot10^{10}$	$1.33\cdot10^{11}$
160	-25	2.007	2.135	$1\cdot10^{-9}$	$1\cdot10^{-9}$	$3.5\cdot10^{-10}$	$4\cdot10^{11}$	$6\cdot10^{-2}$	$1.80\cdot10^{12}$	$7.38\cdot10^{10}$	$2.14\cdot10^{11}$
170	-16	2.007	2.135	$1\cdot10^{-9}$	$1\cdot10^{-9}$	$3.5\cdot10^{-10}$	$4\cdot10^{11}$	$6\cdot10^{-2}$	$2.97\cdot10^{12}$	$1.19\cdot10^{11}$	$3.55\cdot10^{11}$
180	-7	2.007	2.135	$1\cdot10^{-9}$	$1\cdot10^{-9}$	$3.5\cdot10^{-10}$	$4\cdot10^{11}$	$6\cdot10^{-2}$	$7.15\cdot10^{12}$	$2.86\cdot10^{11}$	$8.58\cdot10^{11}$
200	-5	2.007	2.137	$1\cdot10^{-9}$	$1\cdot10^{-9}$	$3.5\cdot10^{-10}$	$4\cdot10^{11}$	$6\cdot10^{-2}$	$1.11\cdot10^{13}$	$4.45\cdot10^{11}$	$1.33\cdot10^{12}$
220	-5	2.007	2.139	$1\cdot10^{-9}$	$1\cdot10^{-9}$	$3.5\cdot10^{-10}$	$4\cdot10^{11}$	$6\cdot10^{-2}$	$1.22\cdot10^{13}$	$4.89\cdot10^{11}$	$1.46\cdot10^{12}$

IV. Comment on Figure 5.

The hardly observable feature around 4.2 T in Fig. 5b (122 GHz) has a different nature than the similar weak signals in Figures 3 and 4. We attribute it to the impurity that often arises in solvent-containing breathing crystals upon aging: the solvent molecules escape from the outer surface of the crystal and thus the structure and magnetic properties of these "solventless" triads change. The proof that this signal is not a line of the other multiplet or other structural state is that we never observe the intensity of this signal to be comparable to the (strong) signal of the spin triad, as opposed to those in figures 3 and 4. Instead, the position and intensity of this impurity signal is temperature-independent as opposed to the behavior of signal of spin triad (Fig.S3) i.e., this weak signal does not participate in the spin dynamics of the system and thus has not to be considered.

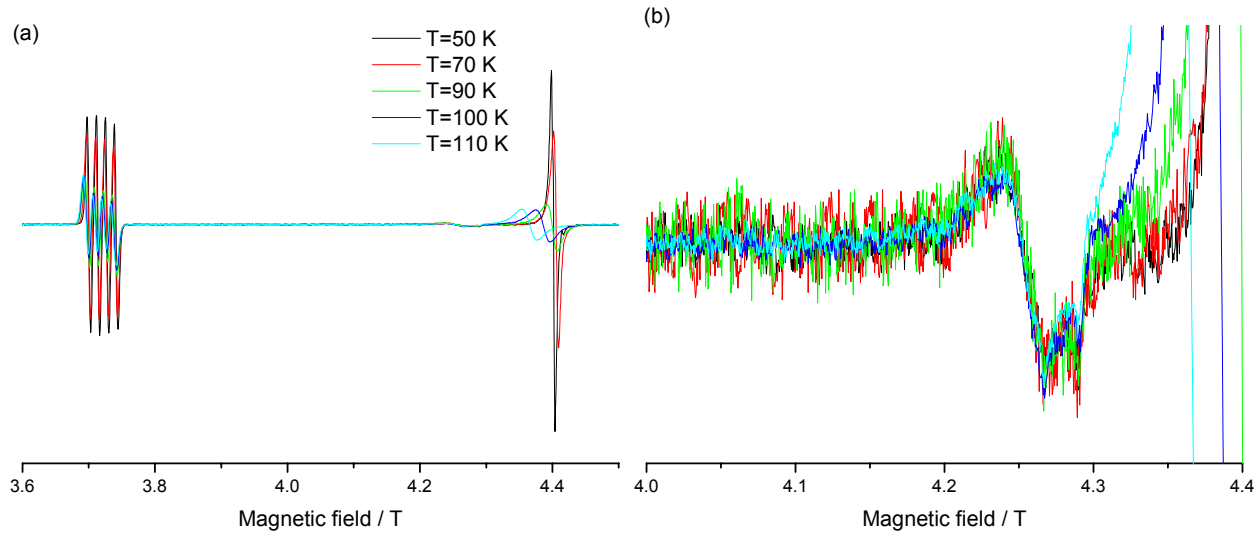

Figure S3. (a) Five upper plots of Figure 5b: Temperature-dependent EPR spectra of $Cu(hfac)_2L^{Bu}\cdot 0.5C_8H_{18}$, $\nu_{mw}\approx 122.00$ GHz. All spectra are normalized to the first integral of signal of one-spin copper ion (low-field part of the spectrum). (b) The same spectra with large magnification of the region with the impurity signal.

V. Crystal data and experimental details for $Cu(hfac)_2L^{Bu}\cdot 0.5C_8H_{10}$

Table. Crystal data and experimental details for $Cu(hfac)_2L^{Bu}\cdot 0.5C_8H_{10}$

Compound	$Cu(hfac)_2L^{Bu}\cdot 0.5C_8H_{10}$					
Formula	$C_{28}H_{30}CuF_{12}N_4O_6$					
M	810.10					
Crystal system	Triclinic					
Space group	*P*-1					
Z	2					
T, K	60	100	150	180	240	295
a,	10.0756(18)	10.086(3)	10.141(2)	10.2433(18)	10.276(2)	10.387(6)
b,	13.044(2)	12.989(4)	12.980(3)	13.051(2)	12.984(3)	13.198(7)
c, Å	13.736(3)	13.689(5)	13.738(3)	13.874(3)	13.880(3)	14.134(8)
α,	99.469(3)	99.323(6)	99.390(3)	99.494(3)	99.10(3)	100.262(8)
β,	103.364(2)	103.599(6)	103.585(3)	103.534(3)	104.02(3)	103.434(9)
γ, °	105.094(2)	104.982(5)	104.953(3)	104.780(3)	104.20(3)	103.705(8)
V, Å^3	1646.5(5)	1635.7(10)	1649.3(6)	1693.0(5)	1694.6(6)	1774.3(17)
D_{calc}, g/cm^3	1.634	1.645	1.631	1.589	1.588	1.516

I_{hkl} coll / uniq	12426 / 6688	6793 / 4621	12371 / 6641	16735 / 6885	6664 / 4787	15812 / 6367
$R_{int.}$	0.0326	0.0180	0.0377	0.0409	0.0396	0.0318
$R1$	0.0422	0.0310	0.0496	0.0495	0.0618	0.0504
$wR2$ $(I > 2\sigma_I)$	0.1020	0.0872	0.1181	0.1174	0.1772	0.1337
$R1$	0.0508	0.0332	0.0625	0.0631	0.0699	0.0736
$wR2$ (all data)	0.1061	0.0884	0.1245	0.1240	0.1867	0.1532

References

[1] M. Fedin, S. Veber, I. Gromov, V. Ovcharenko, R. Sagdeev, E. Bagryanskaya, *J. Phys. Chem. A*, 2007, **111**, 4449-4455.
[2] S. L. Veber, M. V. Fedin, A. I. Potapov, K. Yu. Maryunina, G. V. Romanenko, R. Z. Sagdeev, V. I. Ovcharenko, D. Goldfarb, E. G. Bagryanskaya, *J. Am. Chem. Soc.*, 2008, **130**, 2444-2445.
[3] S. L. Veber et.al. 2009, in preparation.
[4] M. Fedin, S. Veber, I. Gromov, K. Maryunina, S. Fokin, G. Romanenko, R. Sagdeev, V. Ovcharenko, E. Bagryanskaya, *Inorg. Chem.*, 2007, **46**, 11405-11415.